HYDROACOUSTIC AND PHOTOGRAPHIC TECHNIQUES APPLIED TO STUDY THE BEHAVIOR OF KRILL (*Euphausia superba*)

Oscar GUZMAN and Bernardo MARIN

Instituto de Fomento Pesquero, Av. Pedro de Valdivia 2633, P.O. Box 1287, Santiago, Chile

Abstract: During FIBEX expedition to the Antarctic on board of R.V. ITSUMI from Chile, several works were carried out to determine the technical feasibility to use underwater photography combined with hydroacoustic detection techniques, tostudy the behavior of krill (*Euphausia superba*). Several echograms and photographs are presented, showing the results of the works.

Considering the high resolution of the obtained pictures, the calibration of an echo integration constant ($\hat{C}_b$) and mean target strength ($\overline{TS}$) of krill was attempted, to determine the calibrated densities by relating the number of specimens on each photograph with the volume sampled by the camera. The obtained values of $\overline{TS}$ are within the ranges of values estimated by other authors, and the results support the validity and accuracy of this method for the study of the krill behavior.

1. Introduction

During FIBEX expedition to the Antarctic on board of R.V. ITSUMI belonging to the Undersecretariat of Fisheries, Chile, several works were carried out in the surroundings of the Bransfield Strait (Fig. 1) between January 21 and March 2, 1981, to determine the technical feasibility to use underwater photography combined with hydroacoustic detection techniques, to study the behavior of krill (*Euphausia superba*).

The works were performed by the Institute for Fisheries Development (IFOP) with the consultant enterprise Fishing Engineering Ltd. (INGEP), under the sponsorship of the Chilean Antarctic Institute (INACH).

2. Methods and Results

For this purpose, the following photographic (Fig. 2) and hydroacoustic equipments were used:

a) Photographic equipment
   1 underwater photographic camera model 372 Benthos
   1 underwater synchronous flash model 382 Benthos
   1 digital data chamber model 2201 E.P.C.

b) Main acoustic equipment
   1 scientific echo sounder FK-120 Simrad
   1 scientific echo sounder FK-38 Simrad

1 converter QM Simrad
1 analog echo integrator QM-MK-II Simrad
1 hydrophone 8104 Brüel & Kjaer

The electronical calibration of this echo integration system was performed according to the procedures established in the BIOMASS Manual No. 1 on "Calibration of Hydroacoustic Instruments". The main results of this calibration are presented in Table 1.

The photographic camera was lowered into the water by means of an oceanographic winch, to determine its depth at the same time. This measurement was also confirmed through the echo sounder which detected the camera when it overpasses 40 m depth.

Table 1. Results of the echo integration system electronic calibration.

Source level	215.3	(dB/μ Pa ref. 1 m)
Voltage response	−107.8	(dB/1 Vμ Pa)
Gain factor	85	(dB)
Directivity index	24	(dB)
Beam pattern factor	−18	(dB)
Pulse length	0.6	(ms)
Pulse repetition rate	125	(min^{-1})
Echo integrator	45	(mm) (ref. 1 V; 6 min; 10 kt; 30 m channel)

Table 2. Operating conditions of the hydroacoustic and photographic equipment.

a)	Echo sounder EKS-120		
	Frequency	:	120 kHz
	Scale	:	B-0 (0-100 m)
	Power	:	1/1
	Bandwidth	:	wide
	Pulse duration	:	0.6 ms
	T. V. G./Gain	:	20/0
	Sounding ratio	:	125 pulse/min
b)	Echo integrator QM-MK-II		
	Mode	:	3
	Channel A gain	:	10 dB
	Channel B gain	:	10 dB
	Channel A threshold	:	1
	Channel B threshold	:	1
	Channel A depth	:	variable
	Channel B depth	:	variable
	Channels A and B intervals	:	2 m
	Expander	:	×10
	Speed compensator	:	9.0
	Bottom stop function	:	in operation
c)	Underwater photographic camera		
	Lens	:	NIKON f-35
	Focal length	:	37 mm
	Lens opening	:	f 8
	Speed	:	1/20 seg
	Film	:	125 ASA PLUS X

The camera focal field for neatly photographing the krill was determined by suspending dead krill specimens under the lens up to 4.0 m at intervals of 0.5 m. By this way it was established that the optimal focal field of the camera was 2 m starting at 0.5 m from the lens. Also in order to define the photographed surface, the focal angles given by the manufacturer ($\theta_1=35°$; $\theta_2=50°$) were considered. The operating conditions of the hydroacoustic and photographic equipments are given in Table 2.

To obtain the pictures in the acoustically detected krill aggregations, the ship was detained and the camera was lowered into the water. The chronometer of the data back chamber was previously sincronized with that of the ship, in order to determine on the echograms the place where the detected aggregations were photographed.

By this way about 700 positive exposures were obtained, some of which are presented in Figs. 3 to 9, a and b, showing echograms and the most representative pictures taken at several depths and hours of the day.

In spite of the different conditions of time, depth and density of the photographed krill aggregations, it can be observed in Figs. 4b to 9b that the attitude of krill is very similar, with all the specimens gathered swimming with the same corporal orientation. It is slightly different in Figs. 3b and 9b, where the krill found near the surface early in the morning and at night, is more randomly distributed. The maximal density found in the pictures was of 550 exemplars by cubic meter. Special mention must be given to Figs. 3b and 8b where salps were detected.

An attempt was made to photograph a deep scattering layer (Figs. 10a and 10b), where some krill specimens only are possible to detect, probably because the focusing of the camera lens was not appropriate for smaller specimens. In Fig. 6a can be observed also a D.S.L., sampled by means of an IKMT net, catching *Electrona antarctica*, *Gymnoscopelus opisthopterus* and *Protomyctophum bolini*.

Considering the high resolution of the obtained pictures, it was decided to attempt the calibration of the echo integration constant ($\hat{C}_b$) and mean target strength ($\overline{TS}$) of the krill. For this purpose it was necessary to determine the density of photographed exemplars, by relating the number of specimens on each picture with the volume sampled by the camera (GUZMAN *et al.*, 1982).

With the objective to procure that the integrated volume will coincide with the photographed one, channel A of the echo integrator was set with an echo integration interval of 2 m, starting from the camera depth, and channel B was also operated with an echo integration interval of 2 m, programed to integrate from 1 m below the camera depth (Fig. 11).

The initial and final hours of each echo integration sequency, were synchronized with the photographic information adjusting them to the timer included in the camera. From the moment the photographic sequence started, pictures were obtained at the ratio of one per 7 s. In every negative, the exposure and the hour were registered with accuracy of 1 s.

For the calculation of the echo integration coefficient, the data obtained during this calibration were adjusted to a simple linear regression, applying the least squares method and robust estimator, corresponding the independent variable (x) to the integrated millimeters ($\overline{M}$), and the dependent variable (y) to the calibrated densities (ρ_c).

The mean target strength ($\overline{TS}$) was calculated according to the basic equations

proposed by SIMRAD (1972), that derive the $\overline{TS}$ of the calibrated specimens from the mean volume back scattering strength ($\bar{S}_v$).

In Fig. 12 is presented the adjusted regression and in Figs. 13a and 13b, are shown the echograms and some pictures obtained during this calibration. It is very important to observe in Fig. 13b, the high variability of krill density in the short distance (7 m) that separates the pictures (GUZMAN *et al.*, 1982).

The average target strength calculated starting from the calibrated densities was estimated as -65.10 dB, varying from -63.3 dB to -66.9 dB for specimens of $46.0\pm$ 15 mm average length and an individual average weight of 0.57 g (GUZMAN *et al.*, 1982).

With respect to the results of regressions computed to determine the echo integration coefficient, the robust estimator method was considered most proper due the intercept is lower ($\propto = 36.47$ mm). Nevertheless, the results of least squares method were of great usefulness, to verify the regression and accept the likeness hypothesis of the intercept with zero (Ho: $\propto 0$) with $(1-\propto/2)=0.99$.

Considering the above, the echo integration coefficient determined by this method is valid and it also can be proved by means of the $\overline{TS}$ deduced from the same data, whose values are within the ranges of $\overline{TS}$ estimated by other authors for different species of euphausiids.

The similitude of this result with the one obtained by YUDANOV (1981) also during FIBEX, must be emphasized. By applying the direct *in situ* method deduced from densities of krill in the echograms, the following ralation between length and $\overline{TS}$ was established:

$$\overline{TS} = -97.2 + 20.0 \log l.$$

According to this equation, the $\overline{TS}$ for specimens of 46.0 mm reaches -64.0 dB, value that is within the variation range of the photographic calibration.

These results are supporting the validity and accuracy of this method to study the krill behavior. Nevertheless, it can be improved further by using stereoscopic photographic cameras, fitted with data back chambers including a magnetic compass and a reference horizon, to determine the motion sense as well as the tilting angle of the krill.

References

GUZMAN, O., LILLO, S. and MARIN, B. (1982): Calibration of an echo integration constant and mean target strength for antarctic krill (*Euphausia superba*). Symposium on Fisheries Acoustic. Bergen, Norway, June 21–24, 1980.

SIMRAD (1972): Simrad Echo Integrator QM Operation and Maintenance. Including supplement No. C802E for Echo Integrator QM-MK-II. Publication P574E.

YUDANOV, K. I. (1981): Measurements of krill target strength ($\overline{TS}$) during FIBEX. Report of ad hoc Acoustic Working Group. Hamburg, Post-FIBEX Data Interpretation Workshop.

(*Received November 16, 1982*)

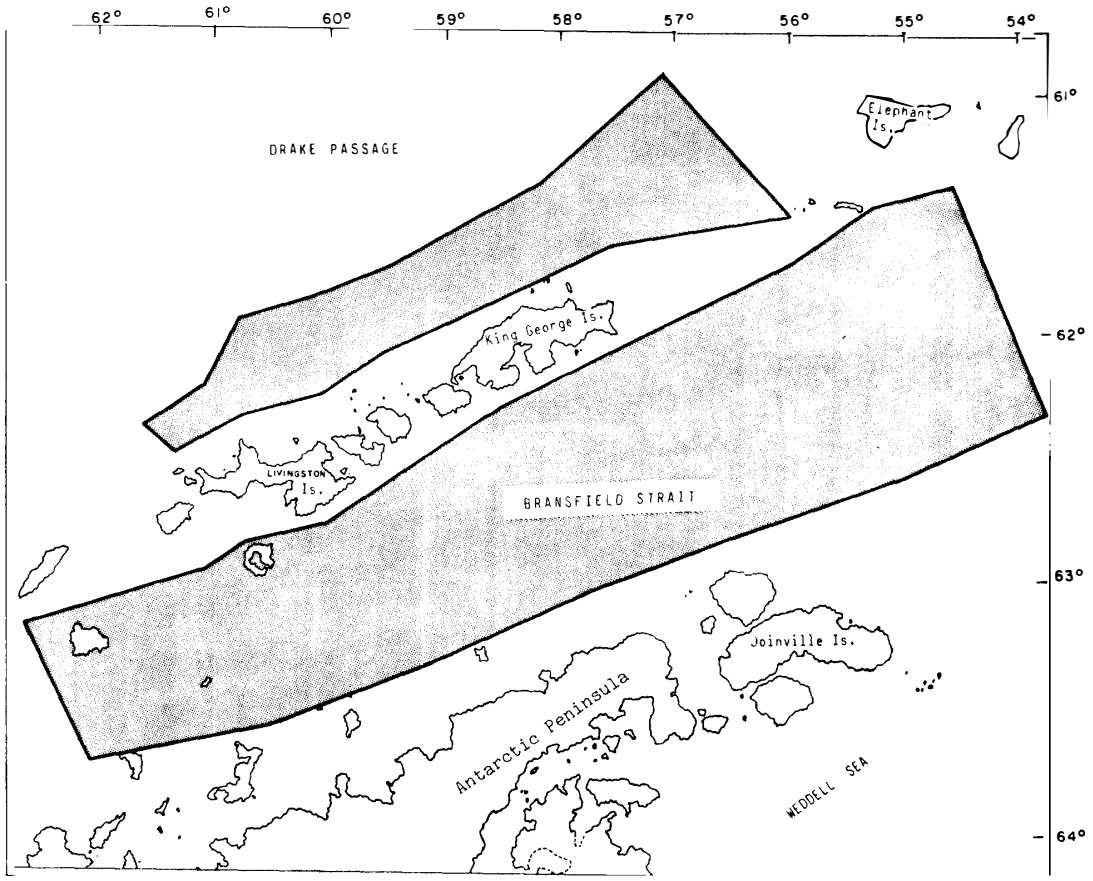

Fig. 1. Areas surveyed by R.V. ITSUMI during FIBEX project (1981).

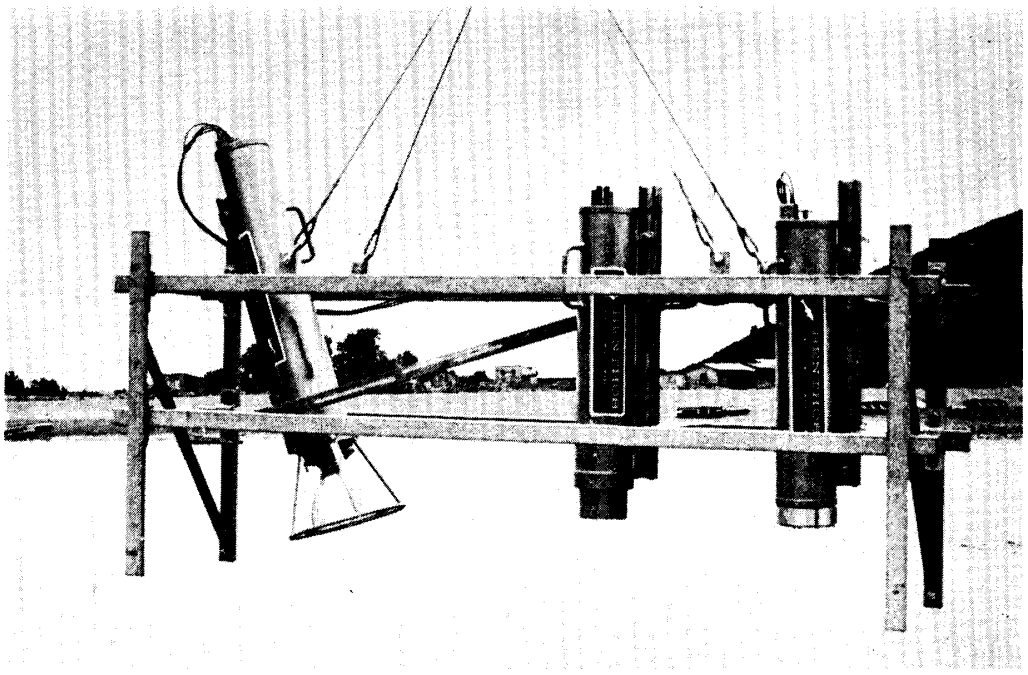

Fig. 2. Underwater camera used during these experiments.

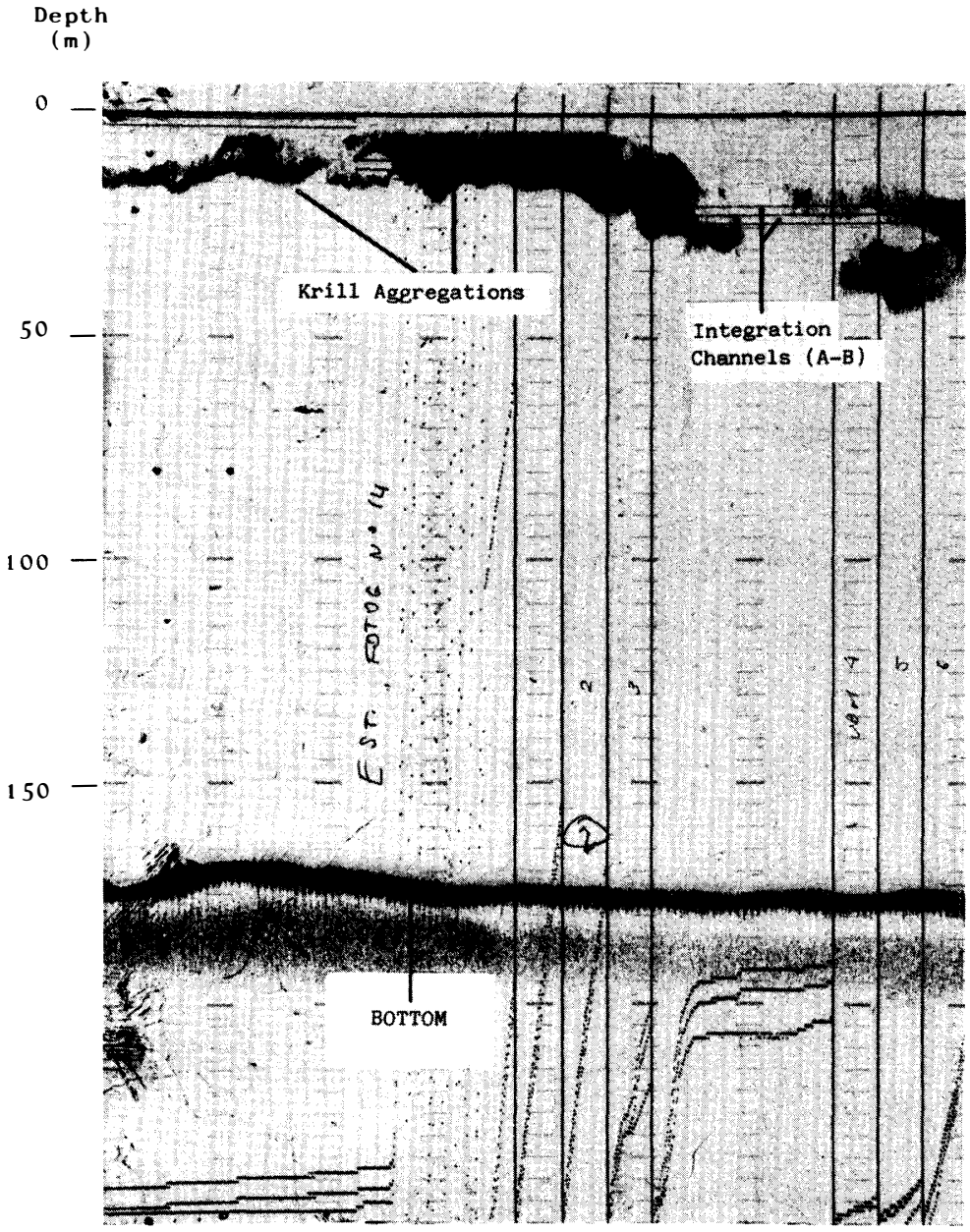

Fig. 3a. Echogram No. 1 with krill aggregations.

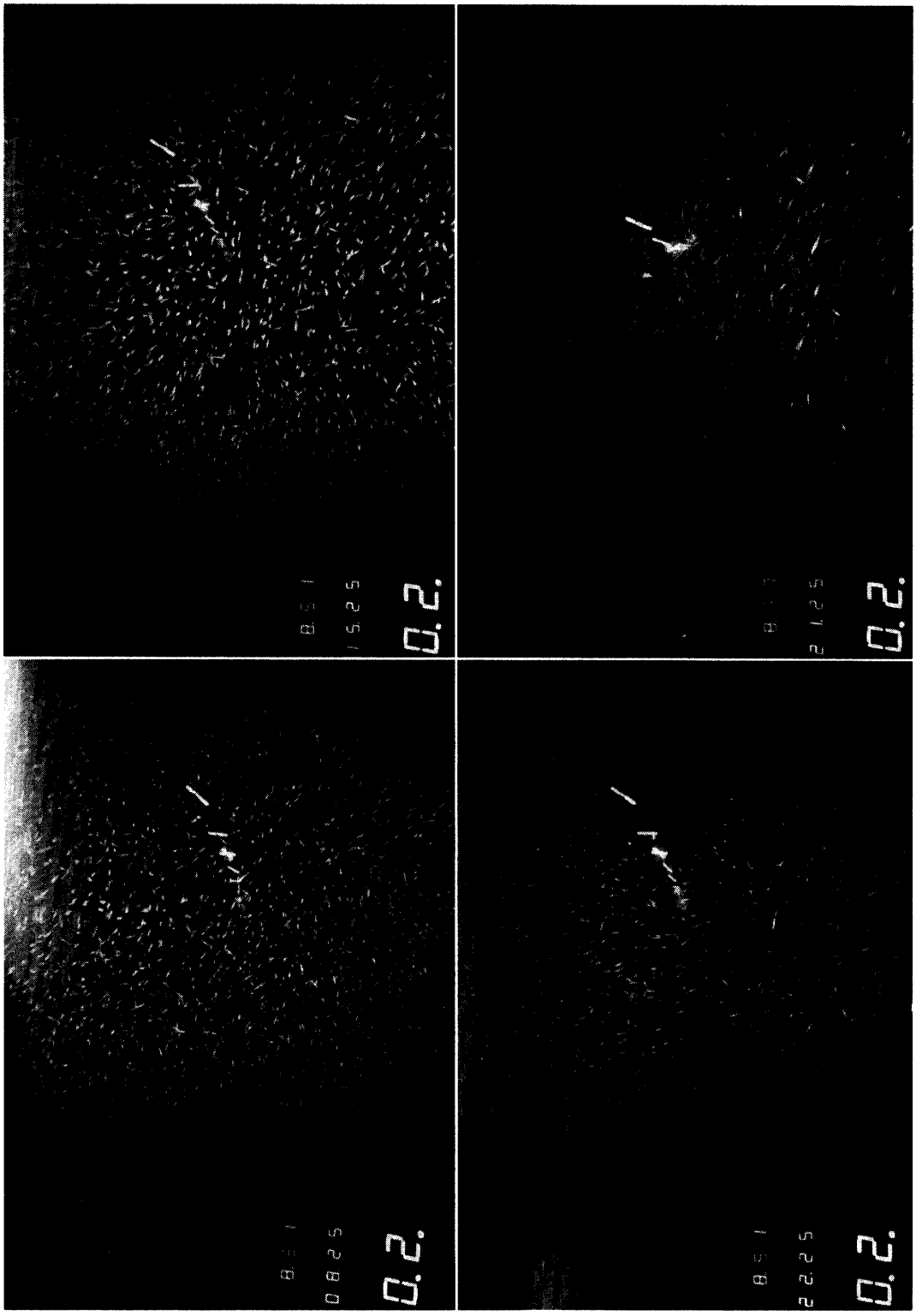

Fig. 3b. Photographs corresponding to echogram No. 1.

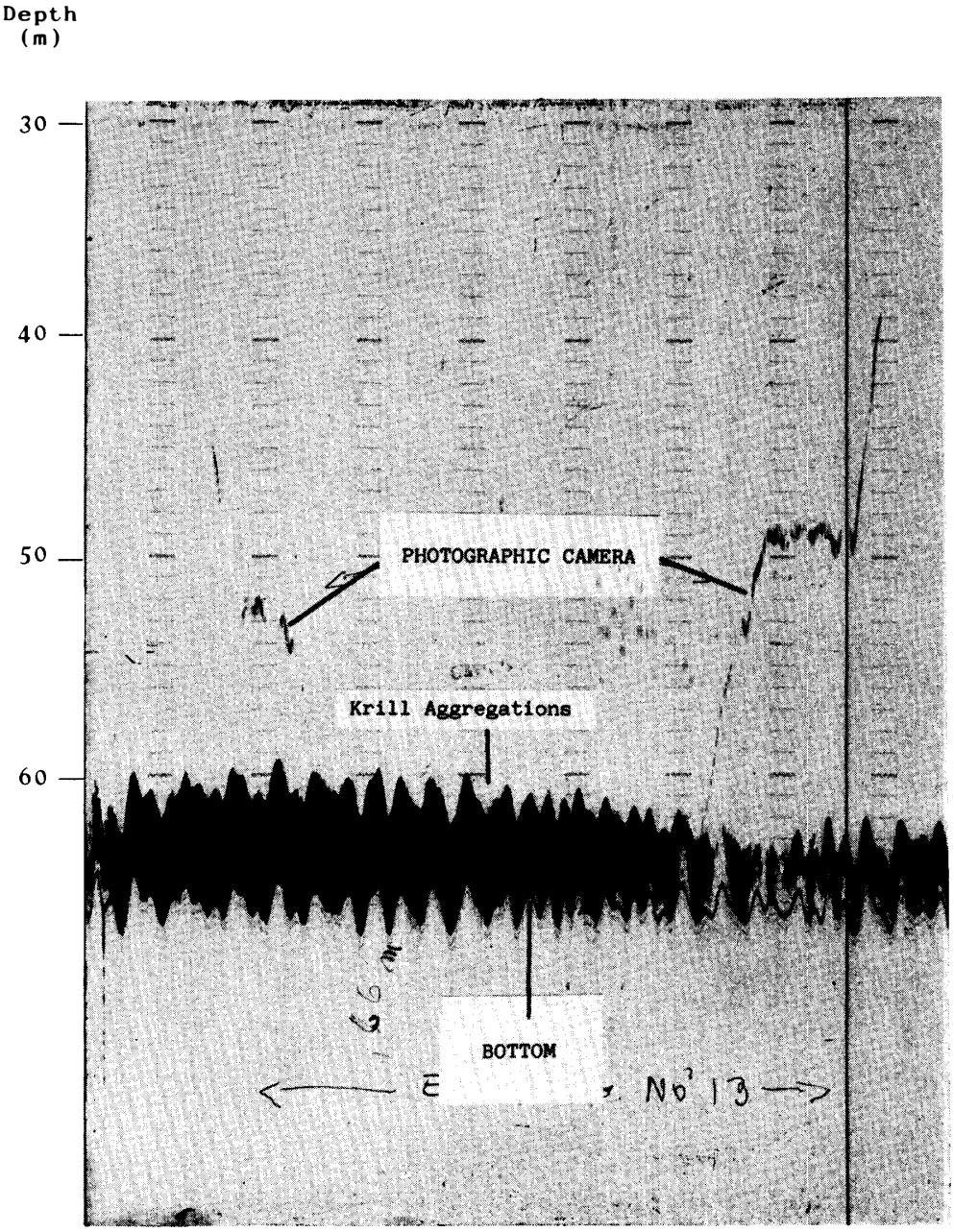

Hour: 10 52 - 10 56 (Local Time)

Fig. 4a. Echogram No. 2 with krill aggregations.

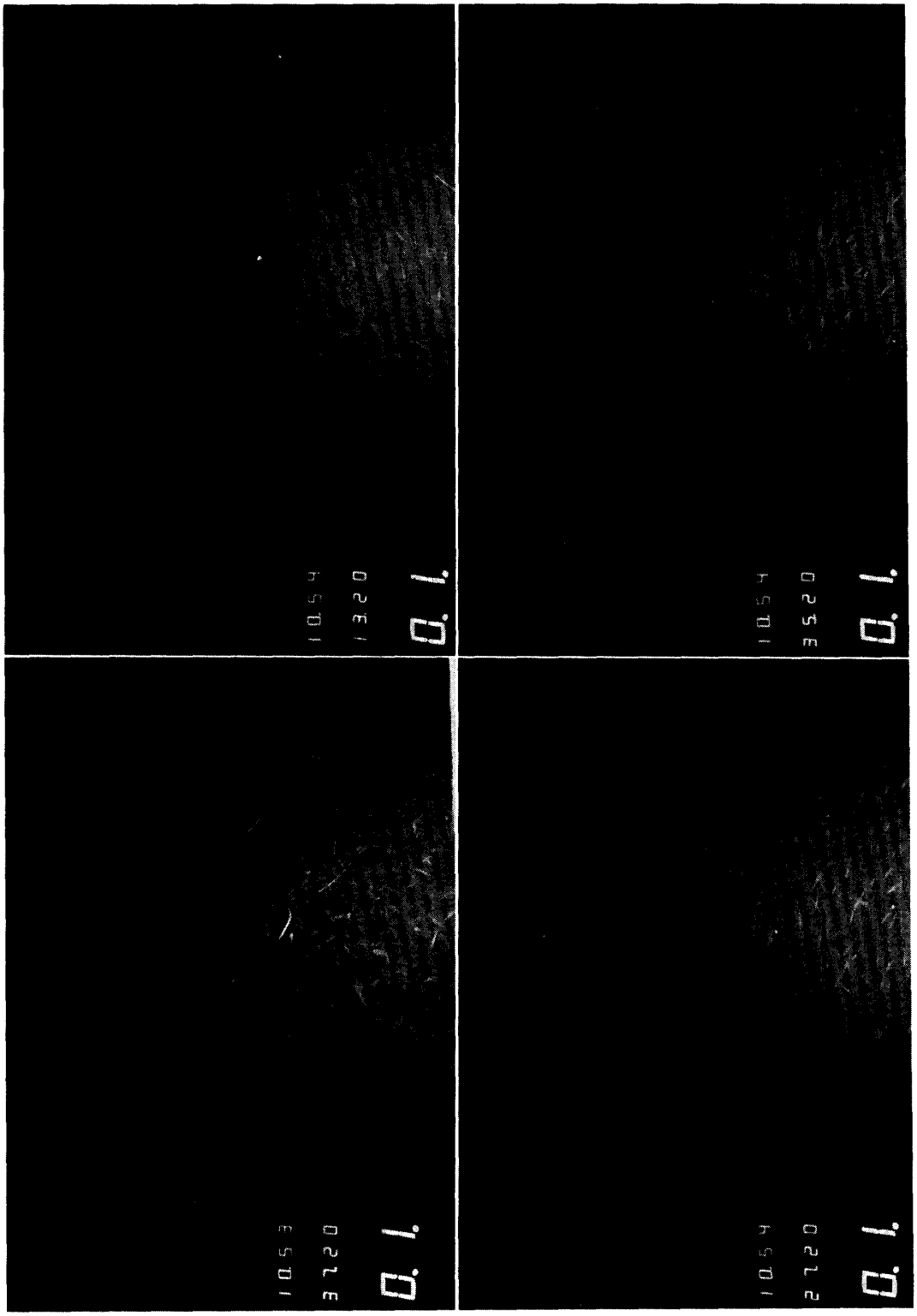

Fig. 4b. Photographs corresponding to echogram No. 2.

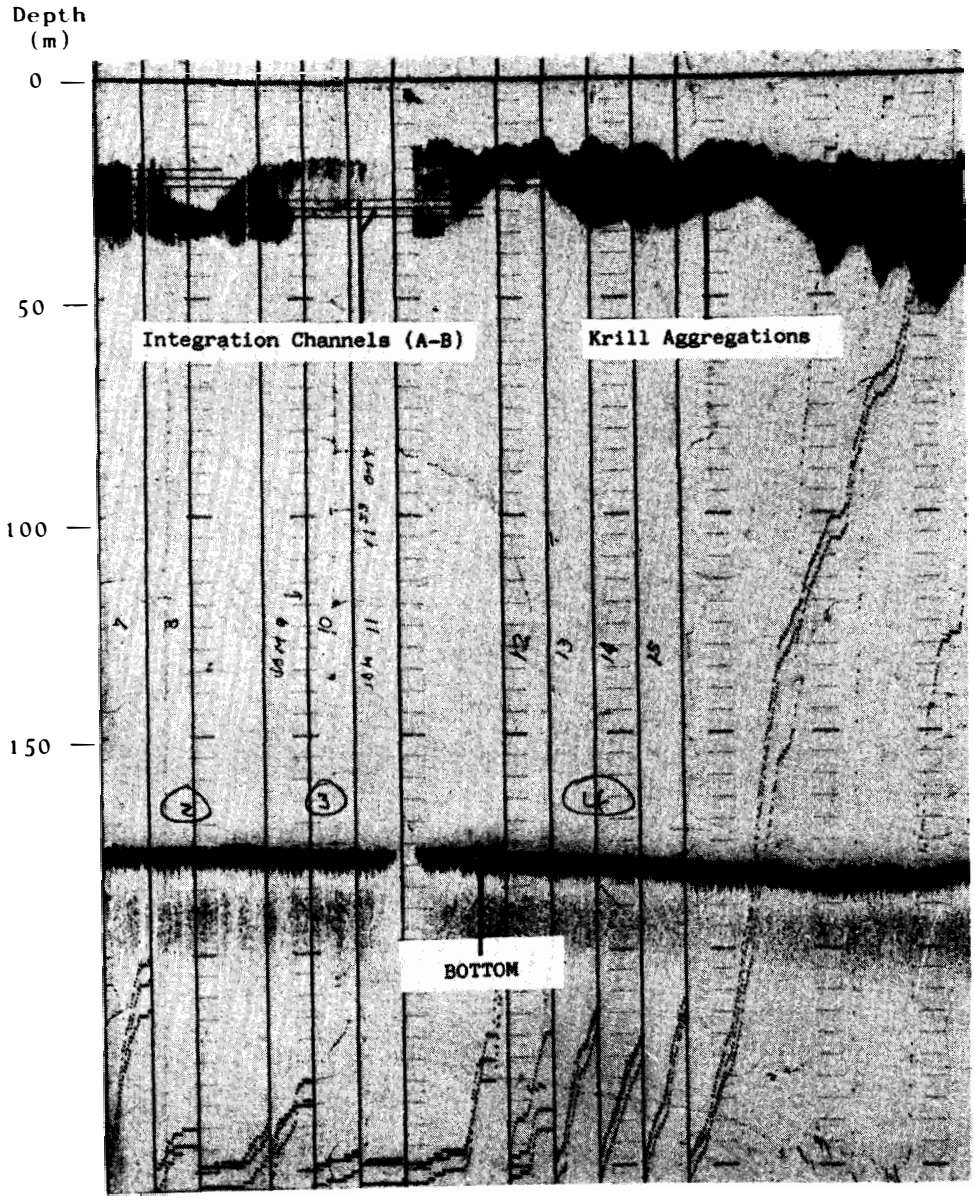

Hour: 11 35 - 11 40 (Local Time)

Fig. 5a. Echogram No. 3 with krill aggregations.

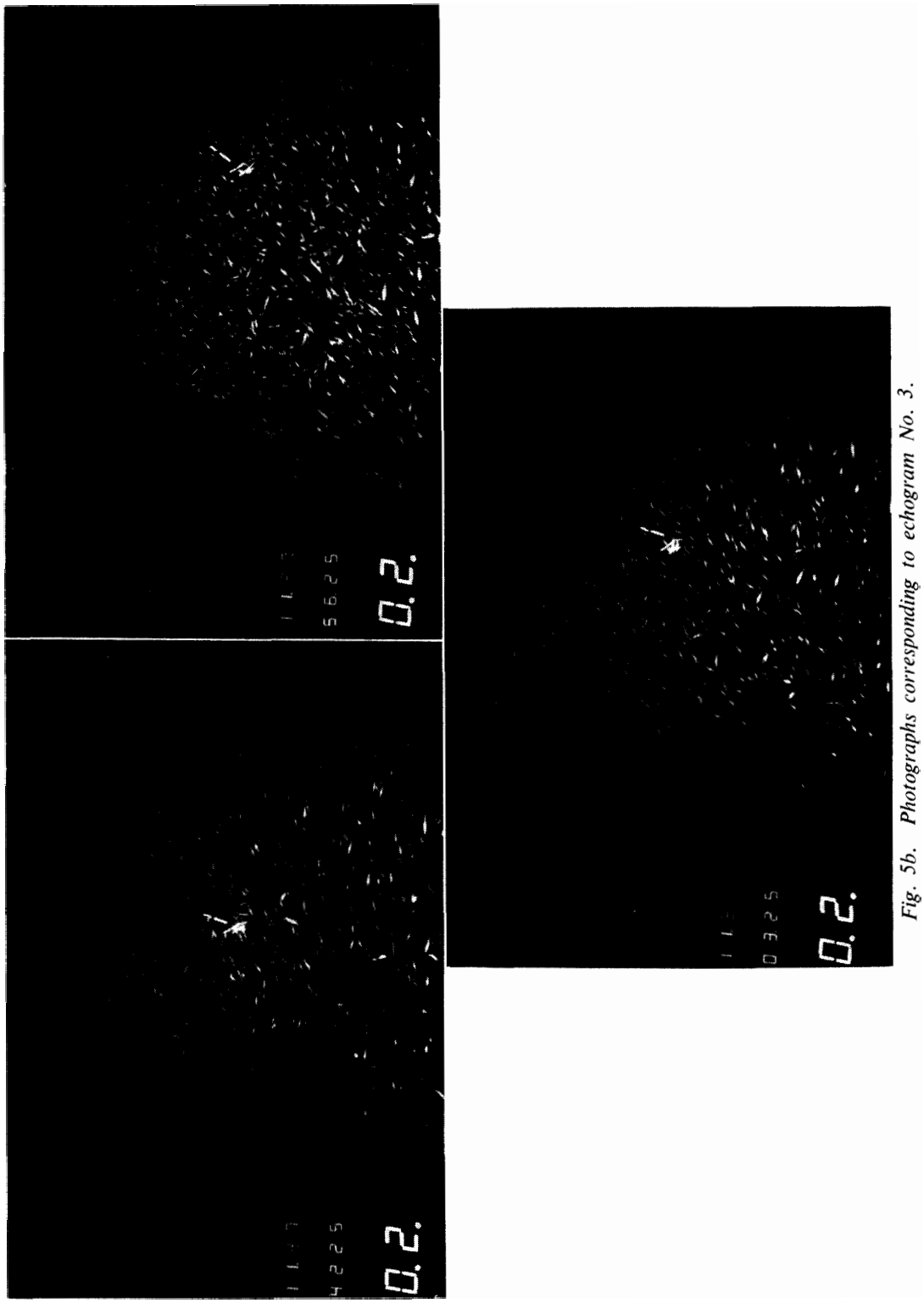

Fig. 5b. Photographs corresponding to echogram No. 3.

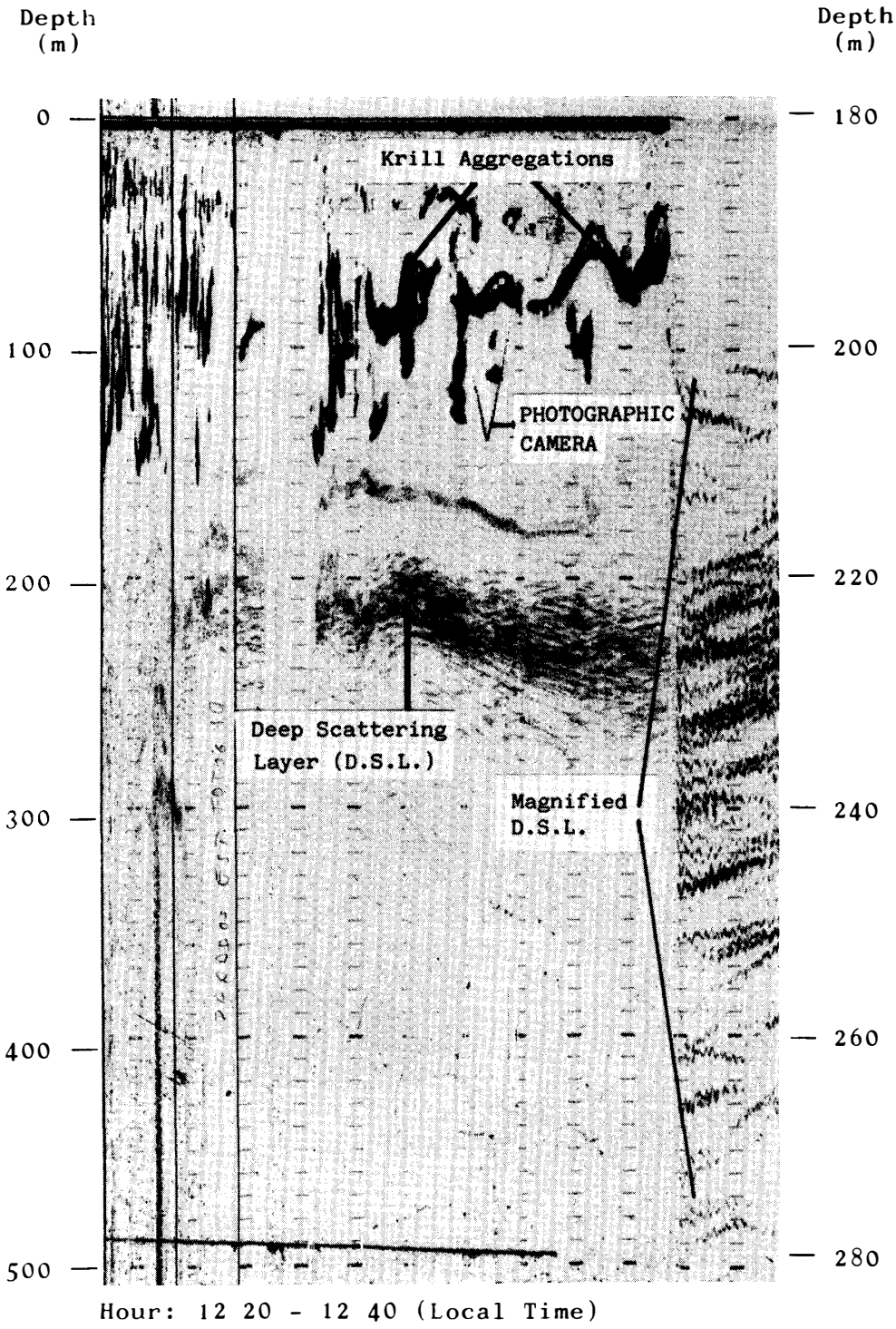

Fig. 6a. Echogram No. 4 with krill aggregations and a Deep Scattering Layer.

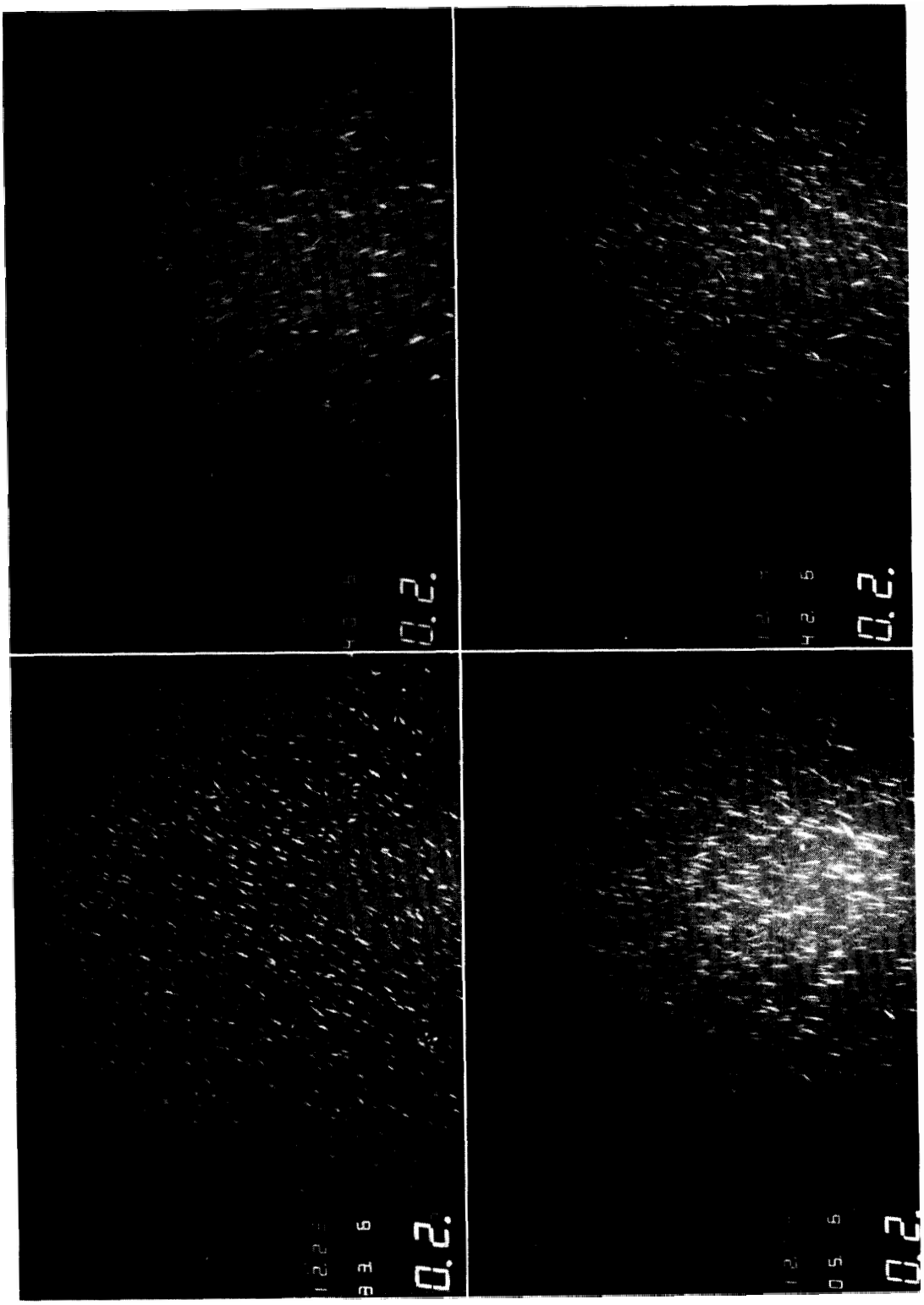

Fig. 6b. Photographs corresponding to echogram No. 4.

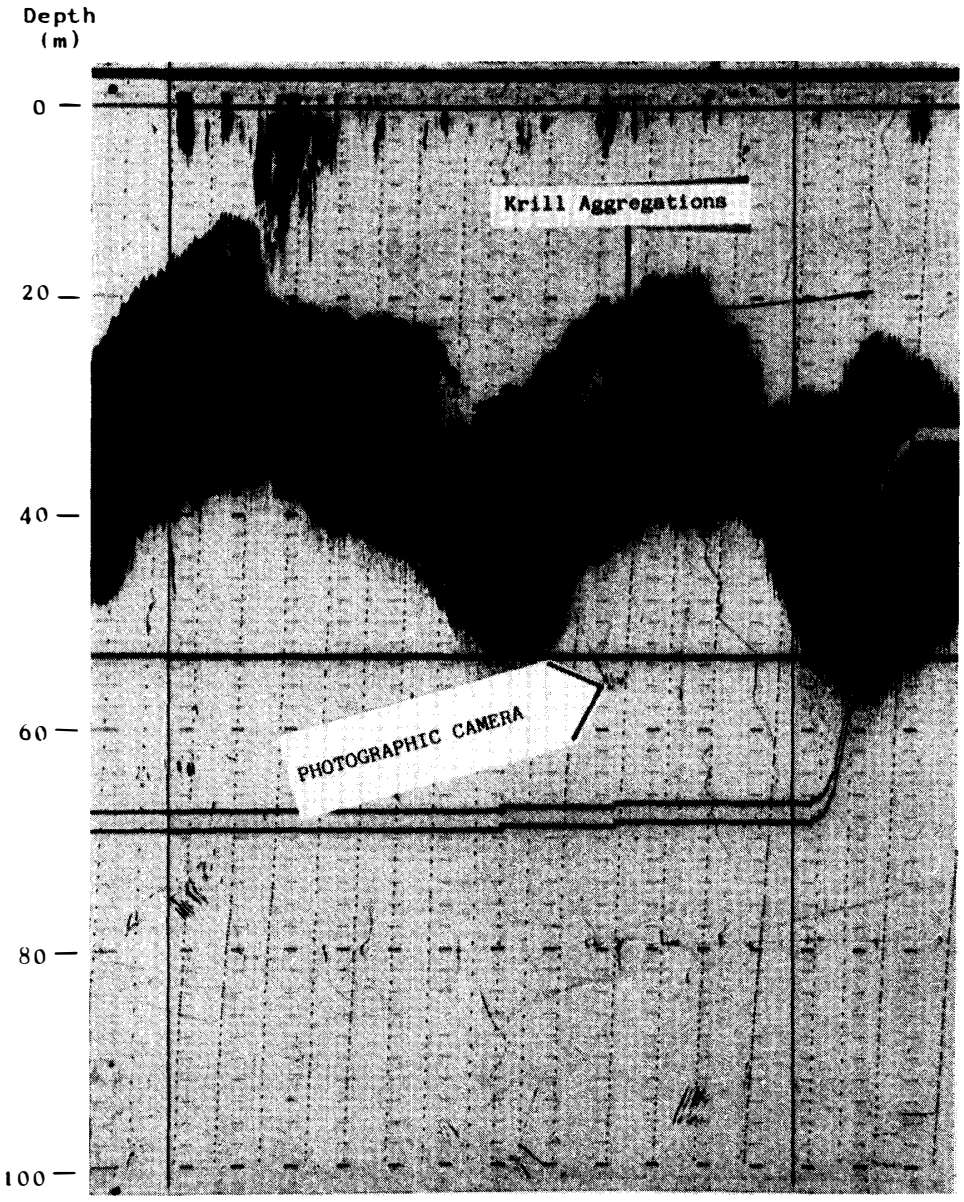

Fig. 7a. Echogram No. 5 with krill aggregations.

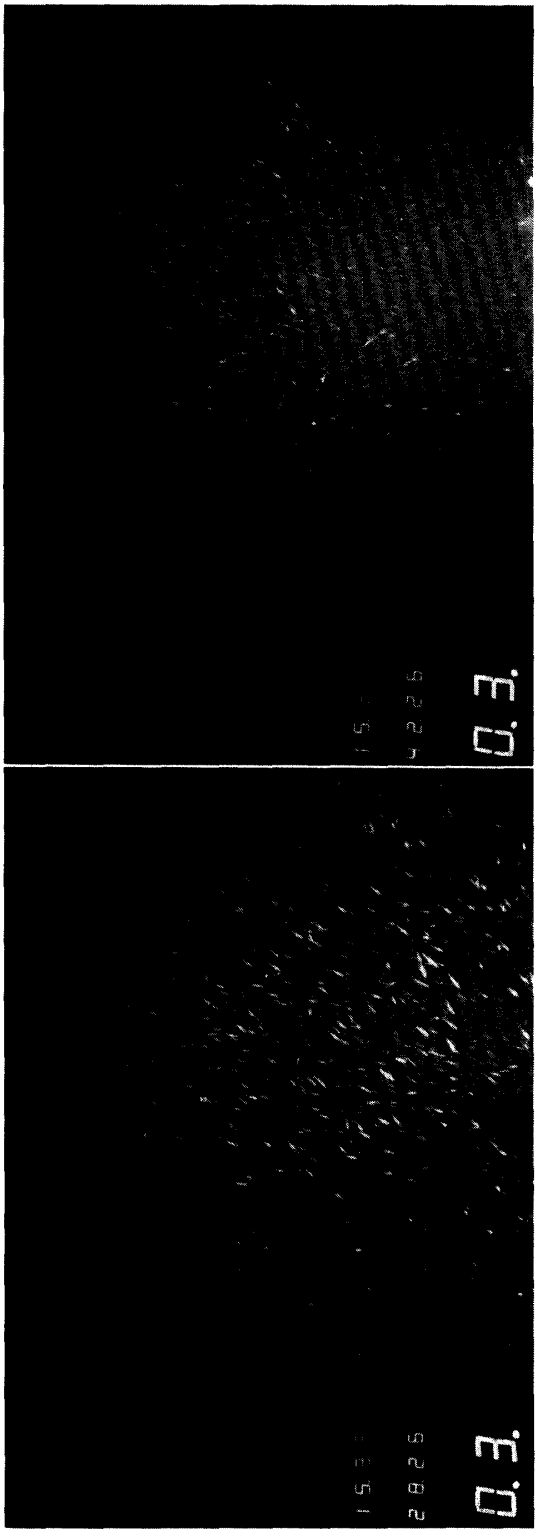

Fig. 7b. Photographs corresponding to echogram No. 5.

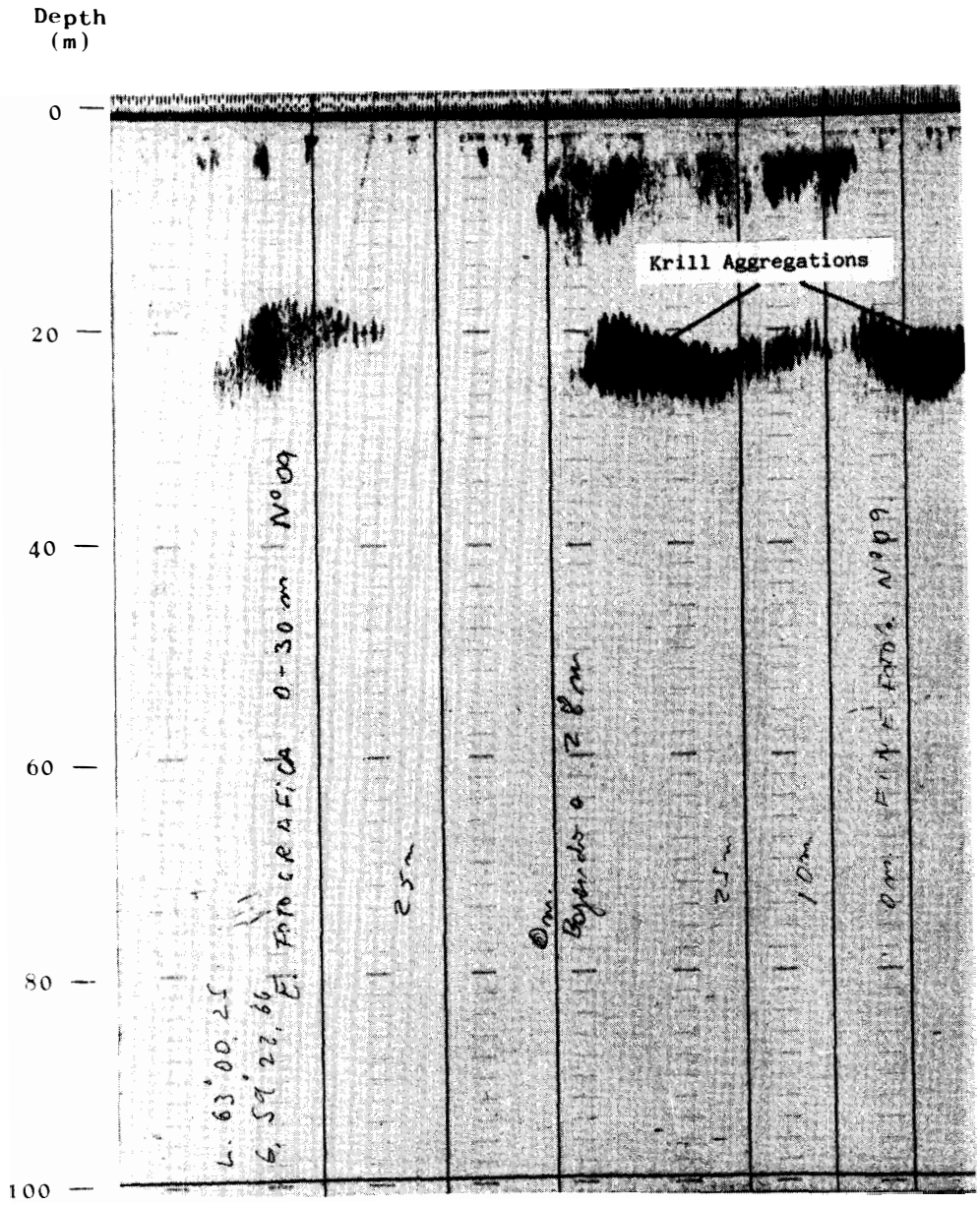

Hour: 17 50 - 17 57 (Local Time)

Fig. 81. Echogram No. 6 with krill aggregations.

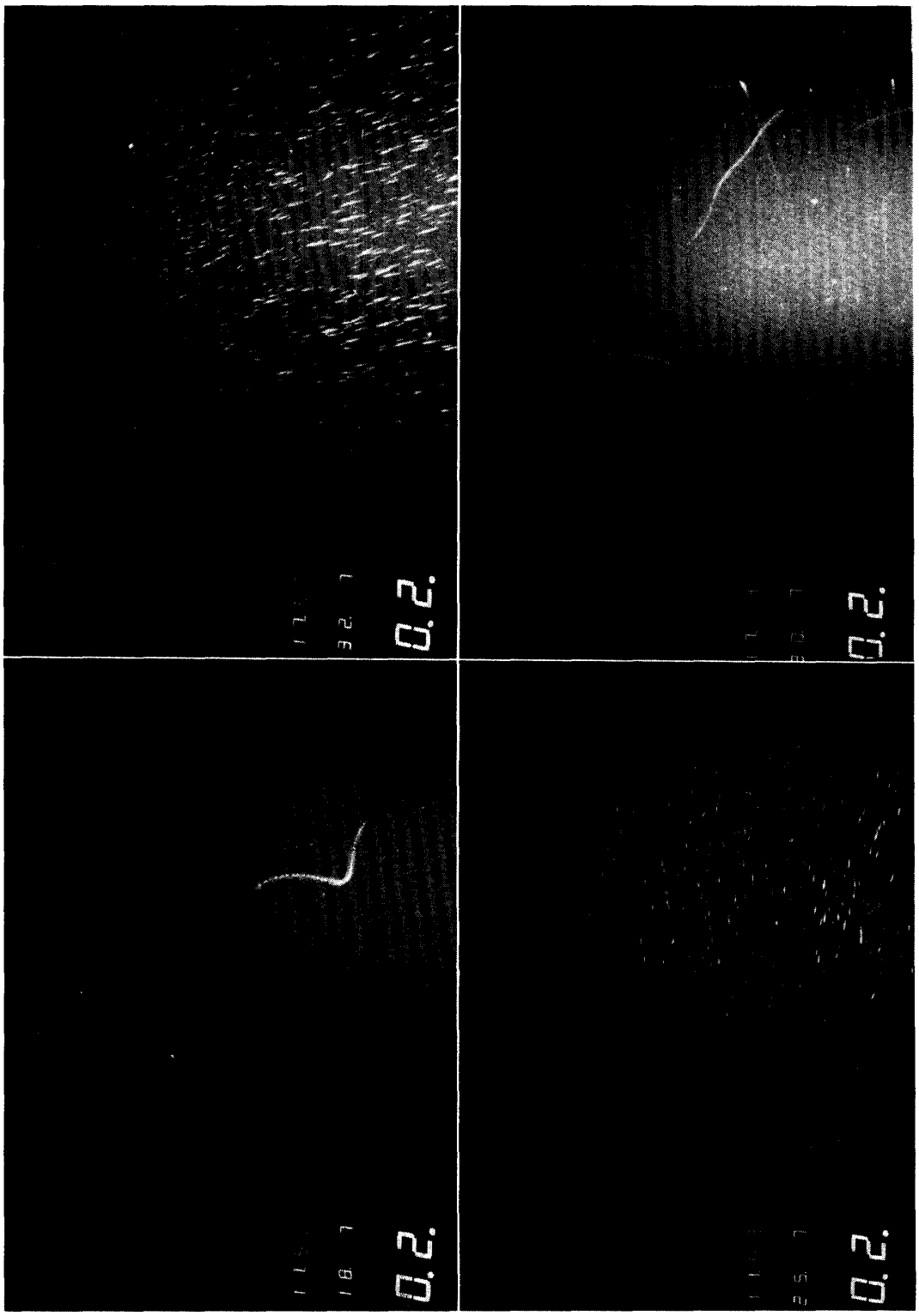

Fig. 8b. Photographs corresponding to echogram No. 6.

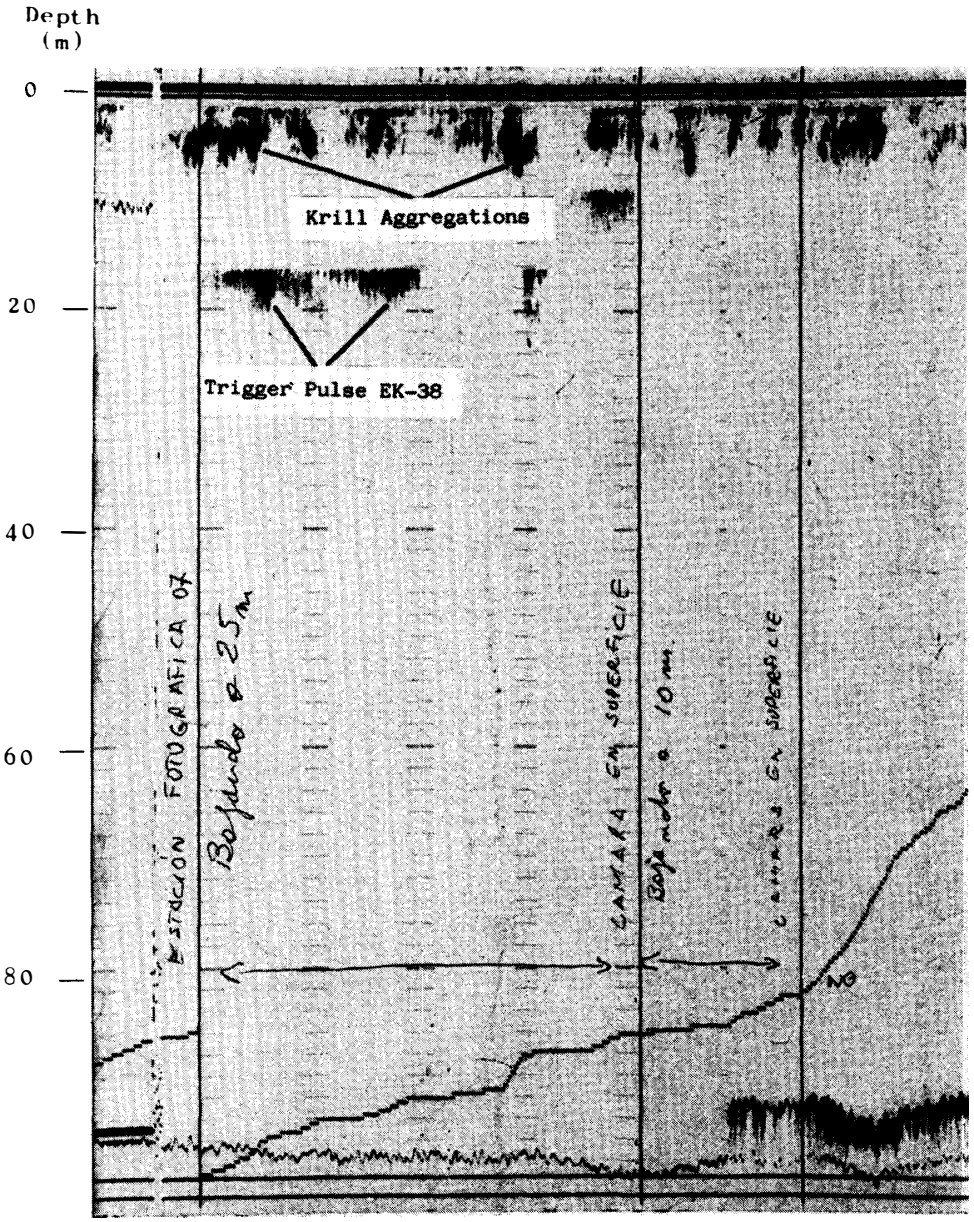

Hour: 20 00 - 20 10 (Local Time)

Fig. 9a. Echogram No. 7 with krill aggregations.

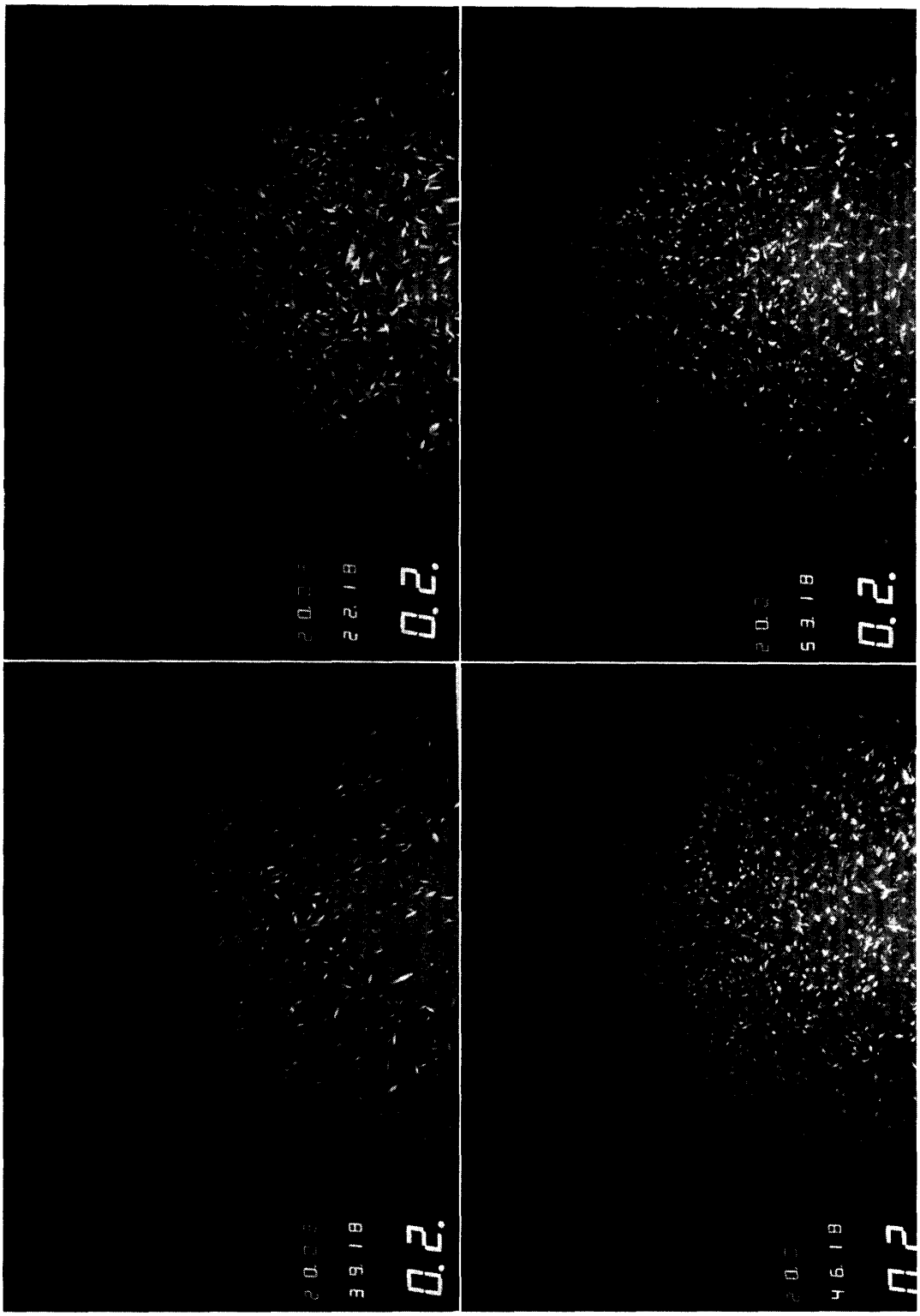

Fig. 9b. Photographs corresponding to echogram No. 7.

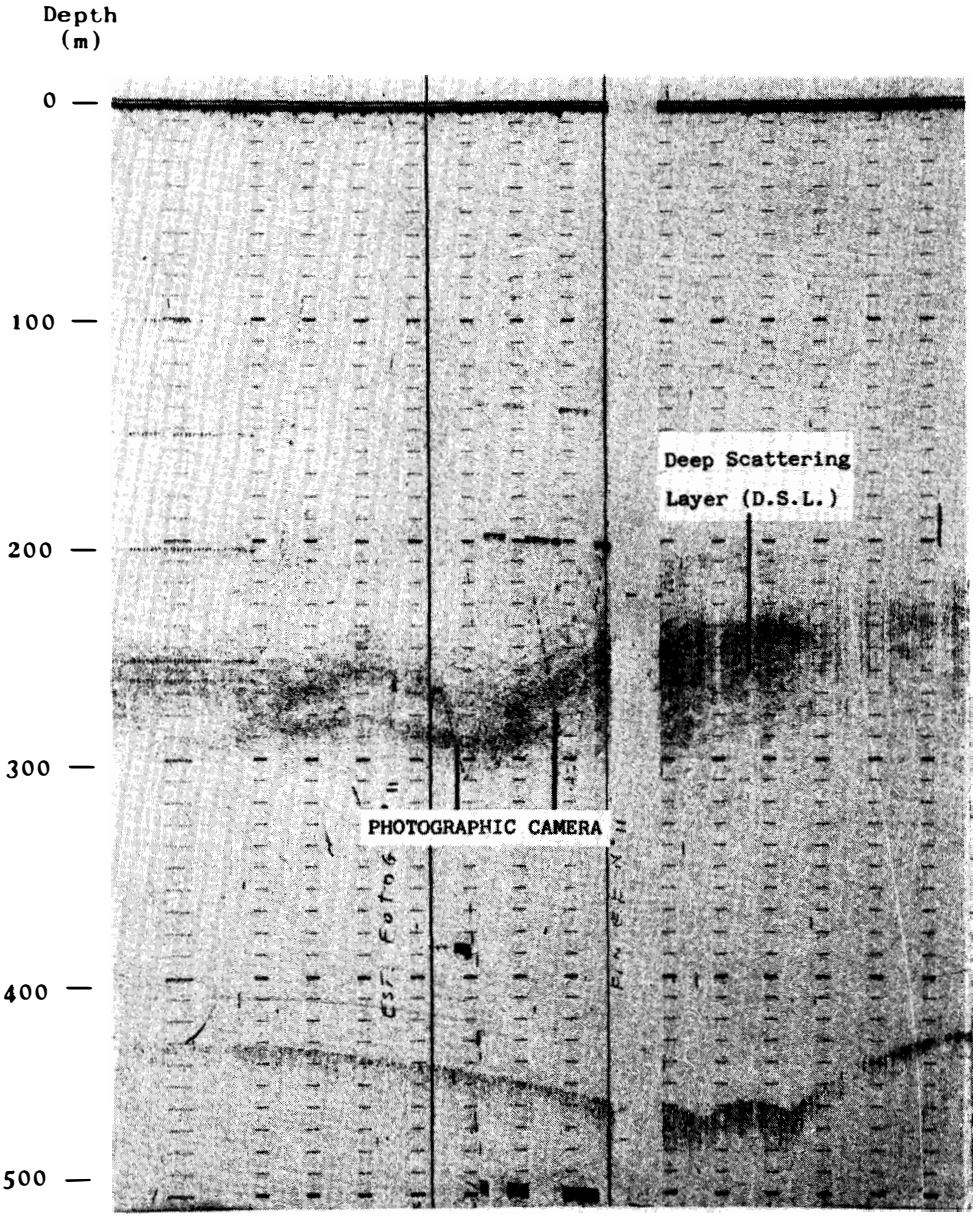

Hour: 10 25 - 10 29 (Local Time)

Fig. 10a. Echogram No. 8 with krill aggregations.

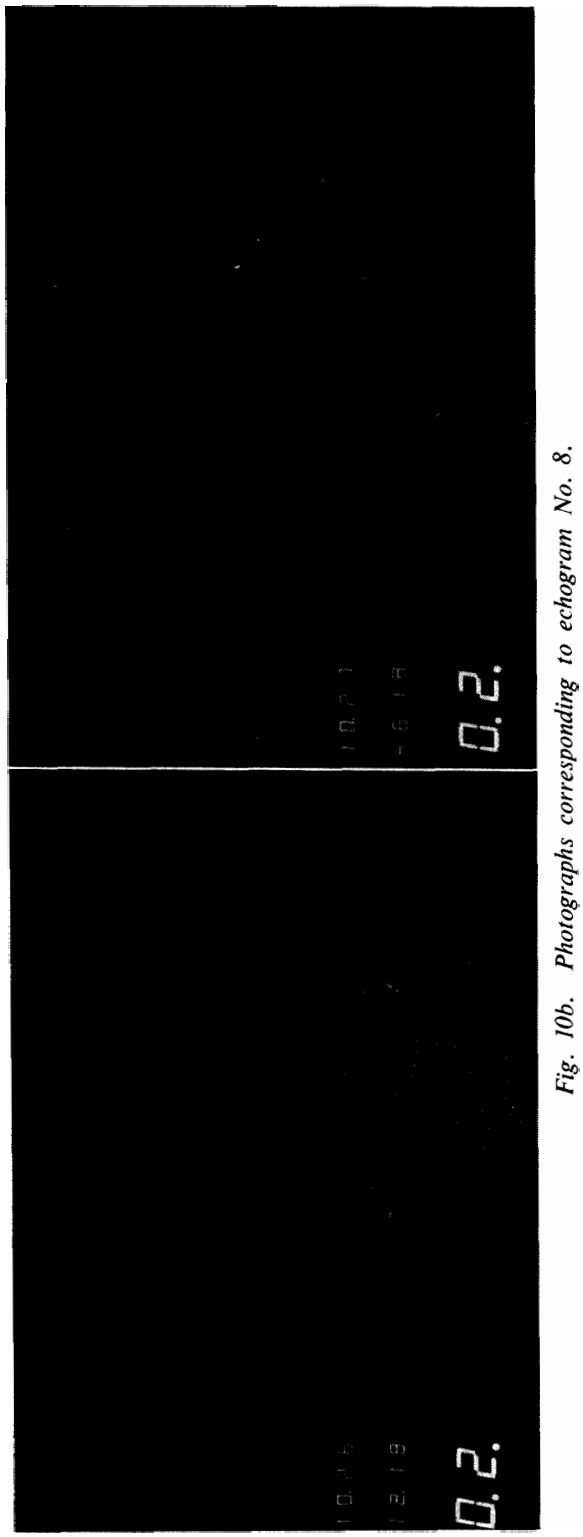

Fig. 10b. Photographs corresponding to echogram No. 8.

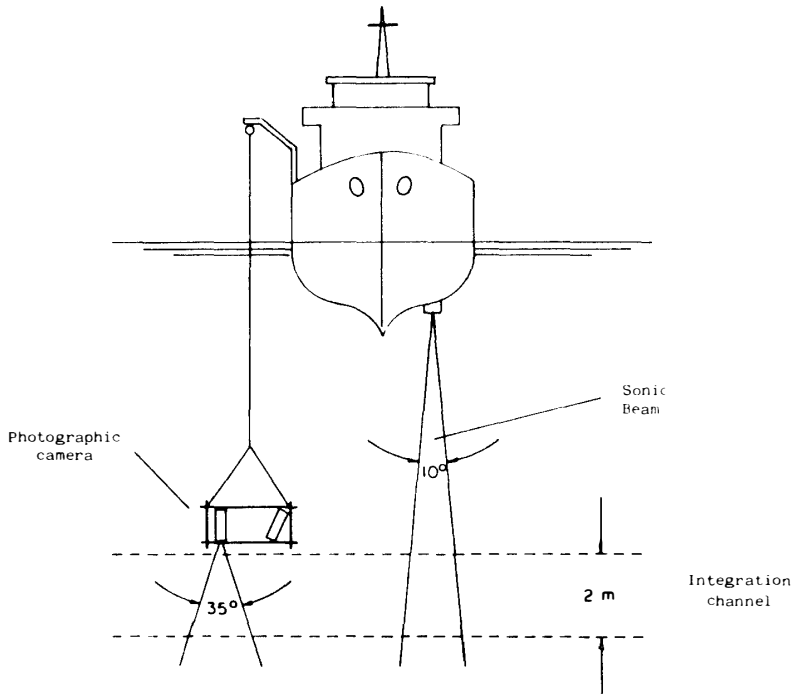

Fig. 11. Scheme of the photographic calibration method.

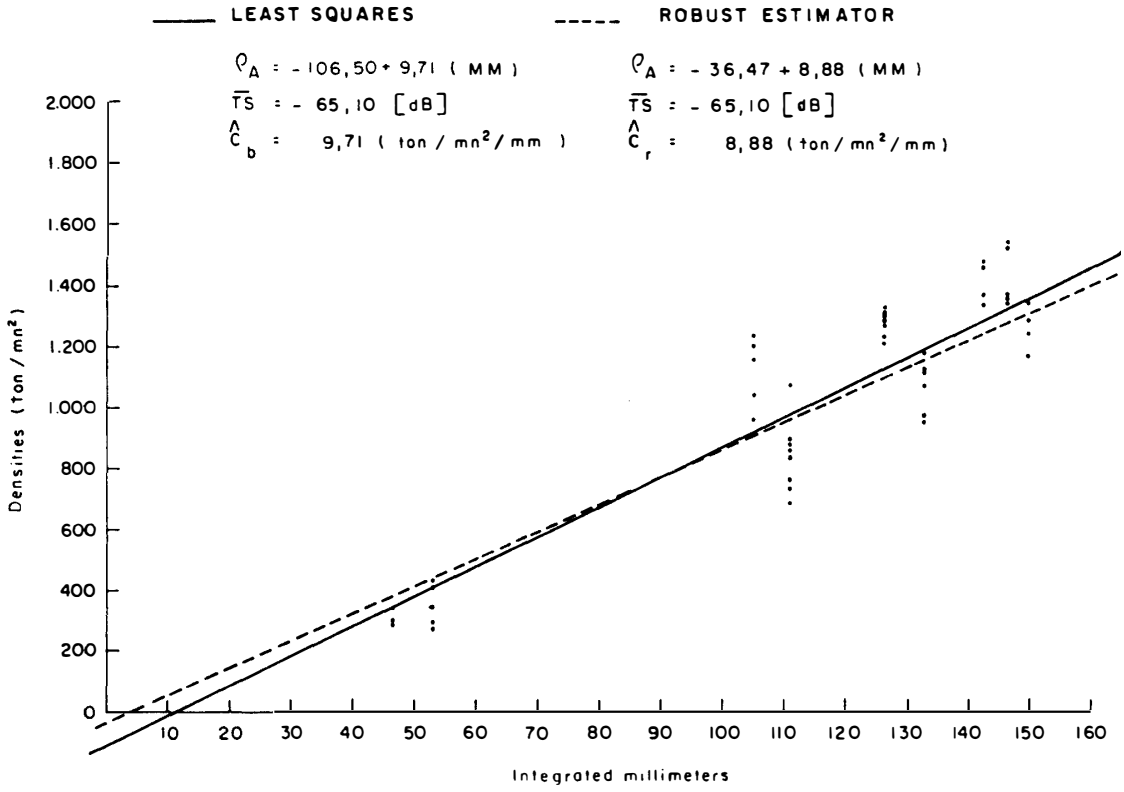

Fig. 12. Functional relationship between the calibrated densities of krill and the echo integrator output (mm).

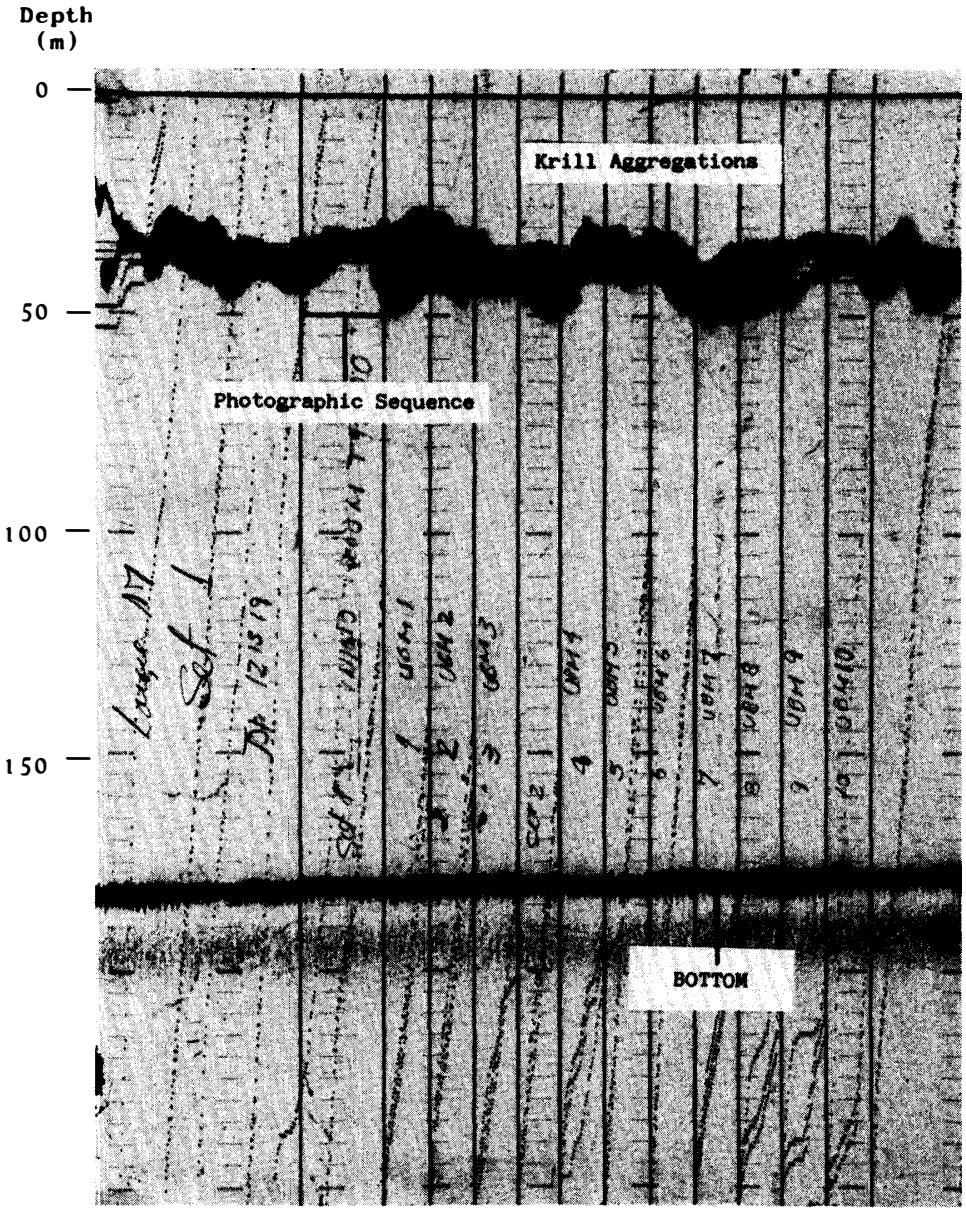

Fig. 13a. Echogram No. 9 with krill aggregations detected during the echo integrator calibration.

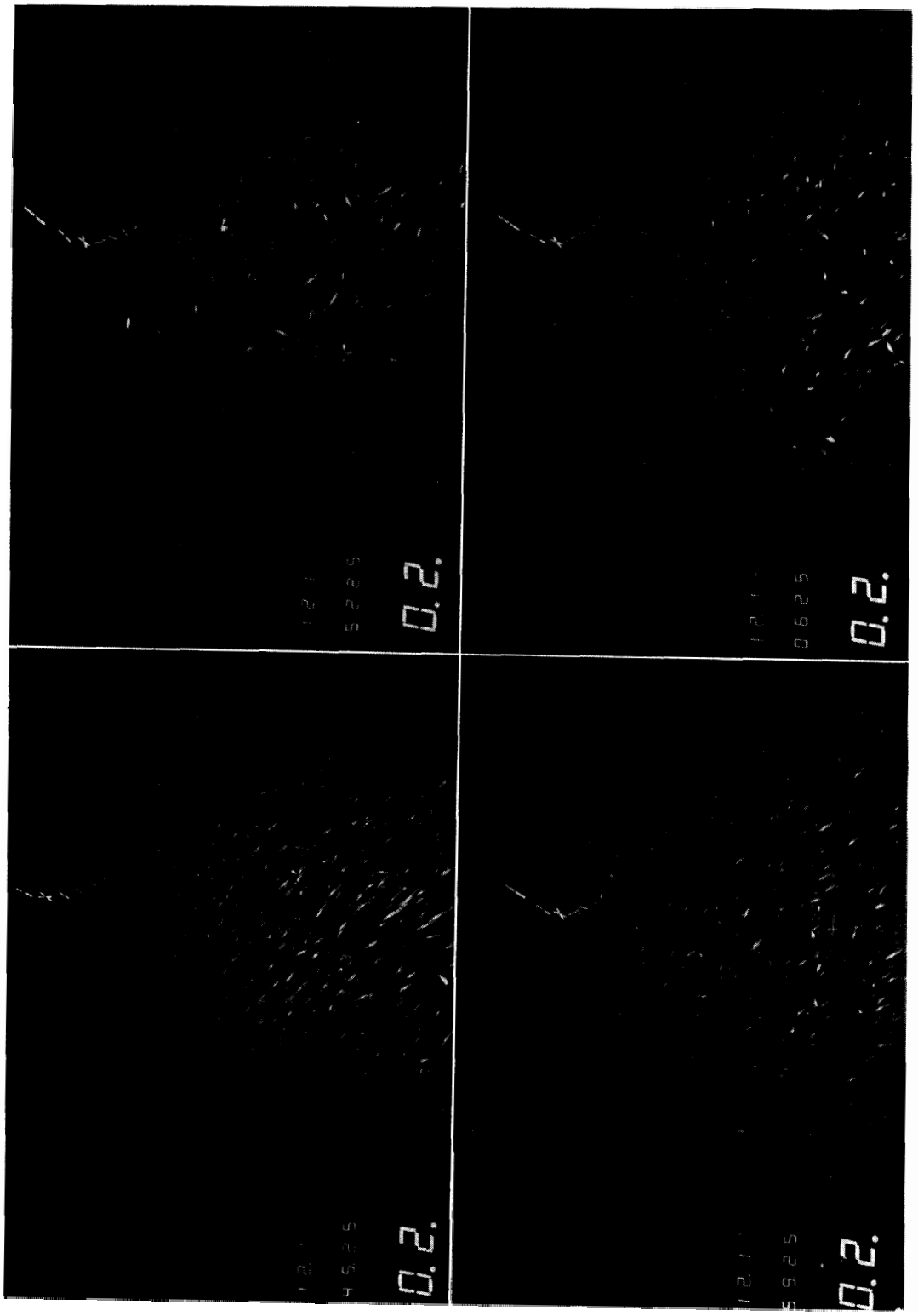

Fig. 13b. Photographs corresponding to echogram No. 9.